Gate dependent photocurrents at a graphene p-n junction

Eva C. Peters, Eduardo J. H. Lee, Marko Burghard, and Klaus Kern

Citation: Appl. Phys. Lett. **97**, 193102 (2010); doi: 10.1063/1.3505926
View online: http://dx.doi.org/10.1063/1.3505926
View Table of Contents: http://apl.aip.org/resource/1/APPLAB/v97/i19
Published by the American Institute of Physics.

Gate dependent photocurrents at a graphene p-n junction

Eva C. Peters,[1] Eduardo J. H. Lee,[1] Marko Burghard,[1,a)] and Klaus Kern[1,2]
[1]*Max-Planck-Institut fuer Festkoerperforschung, Heisenbergstrasse 1, D-70569 Stuttgart, Germany*
[2]*Institut de Physique de la Matière Condenseé, Ecole Polytechnique Fédérale de Lausanne, CH-1015 Lausanne, Switzerland*

(Received 24 June 2010; accepted 28 September 2010; published online 9 November 2010)

We have used scanning photocurrent microscopy to explore the electronic characteristics of a graphene p-n junction fabricated by local chemical doping of a graphene sheet. The photocurrent signal at the junction was found to be most prominent for gate voltages between the two Dirac points of the oppositely doped graphene regions. The gate dependence of this signal agrees well with simulations based upon the Fermi level difference between the two differently doped sections. It is concluded that the photocurrent maps are dominated by the built-in electric field, with only a minor photothermoelectric contribution. © *2010 American Institute of Physics*.
[doi:10.1063/1.3505926]

Graphene has emerged as a novel, highly promising component of nanoscale electric devices. It is a zero-bandgap semiconductor whose electrical transport characteristic can be tuned between p- and n-type by shifting the Fermi level through an external electric field. Graphene-based p-n junctions have recently attracted strong interest, owing to the possibility to investigate interesting phenomena such as the Hall effect[1–4] and Klein tunnelling.[5–9] In addition, they may enable Veselago lensing of coherent electrons.[10] A convenient fabrication method for graphene p-n junctions is chemical doping,[11,12] which involves n-doping of part of the graphene sheet, while its remainder preserves the p-doping character that arises from oxygen and/or water adsorbates. Nonetheless, a detailed understanding of such p-n junctions is still needed in order to realize novel devices. In this letter, we use scanning photocurrent microscopy (SPCM) (Refs. 13–15) to probe the electronic properties of a chemically doped p-n junction in dependence of the Fermi level in the device. Thus far, the origin of the photocurrent generated in carbon nanostructure-based devices has remained controversial. In fact, while some studies have attributed the photoresponse to the built-in electric fields,[15–17] others have favored the role of thermoelectric effects.[18,19] Hence, we have performed a contrasting analysis of the SPCM data in the framework of these two mechanisms.

The present p-n junction devices were fabricated as follows. First, graphene was mechanically exfoliated from a highly oriented pyrolytic graphite (HOPG) crystal,[20] and then transferred onto a silicon substrate covered with a thermally grown, 300 nm thick SiO_2 layer. Individual graphene sheets were located by optical microscopy, and monolayers identified from confocal Raman spectra (λ_{exc}=488 or 633 nm). Source and drain contacts were defined by e-beam lithography and subsequent evaporation of 0.5 nm Ti/25 nm Au. Toward implementing the p-n junction, a window in a 300 nm double layer poly(methylmethacrylate) (PMMA) resist was opened over one half of the graphene sheet. Subsequently, the exposed area was n-doped by immersion in a 5 wt % aqueous solution of poly(ethyleneimine) (PEI) for ~10 min at room temperature, followed by rinsing the sample with pure water and drying under nitrogen flow. Best doping results were obtained with branched PEI (molecular weight 10 kDa). The local n-doping was confirmed by an upshift and narrowing of the G peak, along with a softening and slight broadening of the two-dimensional peak in the corresponding Raman spectrum.[21]

Prior to chemical doping of the partially PMMA covered sheets, the maximum in the resistance (R) versus gate voltage (V_g) plots occurred at a gate voltage between 0 and +80 V, depending on the exposure to the ambient.[22] After n-doping of the sheet half, two maxima emerged in the R versus V_g plots, as exemplified by Fig. 1. While one maximum was located at roughly the same positive gate voltage as before doping, the other one occurred within the negative gate voltage range, consistent with the behavior of other chemically doped graphene p-n junctions.[12,23] For the specific device in Fig. 1, the charge neutrality points are reached at a back-gate voltage of $V^{Dirac}_{uncovered}$=−10 V for the uncovered (n-doped) region, and $V^{Dirac}_{covered}$=20 V for the covered (p-doped) region. These values correspond to an electron density of 7.5×10^{11} cm^{-2} in the n-doped half, and a hole den-

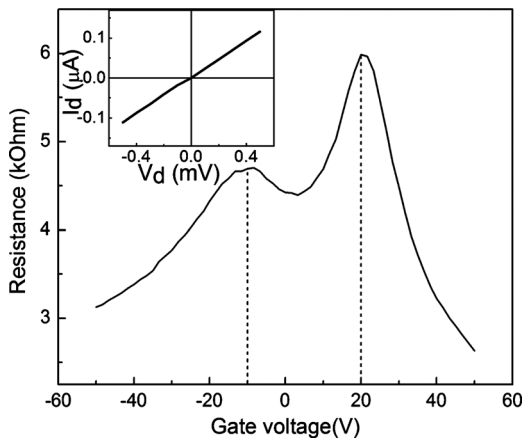

FIG. 1. Transfer characteristic of a graphene pn-junction recorded under ambient. The resistance data were extracted from linear fits to I-V characteristics measured at varying back gate voltage. The two resistance maxima corresponding to the Dirac points occur at $V^{Dirac}_{uncovered}$=−10 V and $V^{Dirac}_{covered}$=20 V. The inset shows the corresponding I-V trace of the device.

a)Author to whom correspondence should be addressed. Electronic mail: m.burghard@fkf.mpg.de.

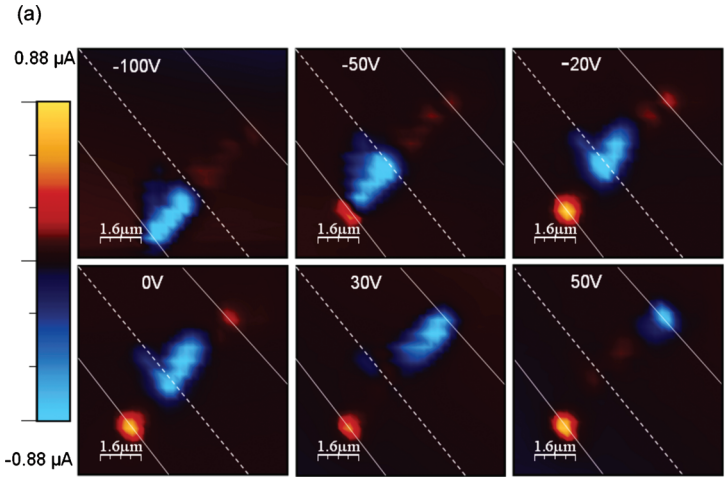

FIG. 2. (Color) Scanning photocurrent microscopy maps of the p-n junction device in Fig. 1. (a) Zero source-drain bias SPCM images acquired at different gate voltages between −100 and +50 V. (b) Optical reflection image of the device with source (S) and drain (D) contacts. The electrode edges are highlighted by solid lines. The n-doped region is located within the lower left quadrant, as denoted by the dopant PEI, while the interface between the PMMA-covered and -uncovered regions appears as diagonal feature (marked by dashed solid line) between the source and drain contact.

sity of 1.5×10^{12} cm^{-2} in the p-doped half, respectively.[20] As expected from theory[5] and confirmed experimentally at low temperature (4 K),[23] the current –voltage (I-V) curves (see inset of Fig. 1) did not show diode behavior, which can be explained by the absence of a band gap and the presence of Klein tunneling.[5–9] Another noteworthy feature is the conduction asymmetry for the two charge carrier types, which is manifested in a lower slope of the hole branch, as compared to the electron branch. This observation can be ascribed to an imbalanced carrier injection from the metal contacts.[11] The asymmetry was found to persist for up to 3 h upon storage of the devices under ambient, whereas it took close to 20 h for the Dirac point to shift back to positive gate voltages. It thus follows that the doping is air stable for at least 3 h.

SPCM measurements were carried out under ambient conditions at zero source drain bias by using a confocal laser microscope (HeNe laser with 633 nm wavelength, ~0.4 μm spot size, and power density of 100 kW per cm^2). Similar SPCM images were obtained with other laser wavelengths (476 or 514 nm from Ar laser), although the magnitude of the photocurrent varied slightly due to the difference in the respective laser power densities. As the transfer curves displayed a significant hysteresis, the gate voltage was swept prior to each SPCM measurement in order to ensure that the device remains within the same hysteresis branch. Before the p-n junction formation, the SPCM images exhibited two major features characteristic of pristine graphene.[15] These are (i) strong photocurrents of opposite sign at the metal contacts which inversed sign upon switching the device from the n- to the p-regime or vice versa, attributable to the presence of potential steps at the metal-graphene interface,[15,24] and (ii) at the Dirac point weak local signals appearing over the sheet, which originate from electron-hole puddles and/or defects. The absence of additional features signifies that the PMMA layer covering part of the graphene sheet by itself does not influence the potential distribution in the device, e.g., via local doping or mechanical deformation of the sheet.

Figure 2 displays a sequence of zero bias SPCM images of the p-n junction device in Fig. 1 recorded at different back gate voltages. For gate voltages close to $V_g=0$ V, intense signals of identical sign occur at the source and drain contact, whose magnitude is comparable to those in pristine graphene devices. Moreover, a similarly strong signal emerges around the p-n junction. Upon sweeping the gate voltage from between the two neutrality points ($V_{\text{midpoint}}=5$ V in Fig. 1) to more negative gate voltages, the junction lobe moves toward the source contact. Conversely, when moving into the more positive gate voltage regime, this lobe shifts in the opposite direction toward the drain contact. The strongest response at the junction occurs at $V_{\text{midpoint}}=5$ V, with the value of approximately −0.9 μA being comparable to the magnitude of the contact responses at $V_g=50$ V.

In Fig. 3(a), the photocurrent detected at the p-n junction is plotted against the applied back gate voltage. To elucidate the mechanism of photocurrent generation, we first consider the gate-dependent Fermi level shift within the two differently doped sheet sections. To this end, the Fermi level position in the two differently doped regions of the sheet is estimated using the relation

$$E_F=\hbar v_F\,\mathrm{sgn}(V_g-V_g^{\text{Dirac}})(\pi\alpha)^{1/2}(V_g-V_g^{\text{Dirac}})^{1/2}, \qquad (1)$$

where the gate coupling parameter $\alpha\sim7.3\times10^{10}$ cm^{-2} V^{-1} relates the electrostatically induced carrier density to the

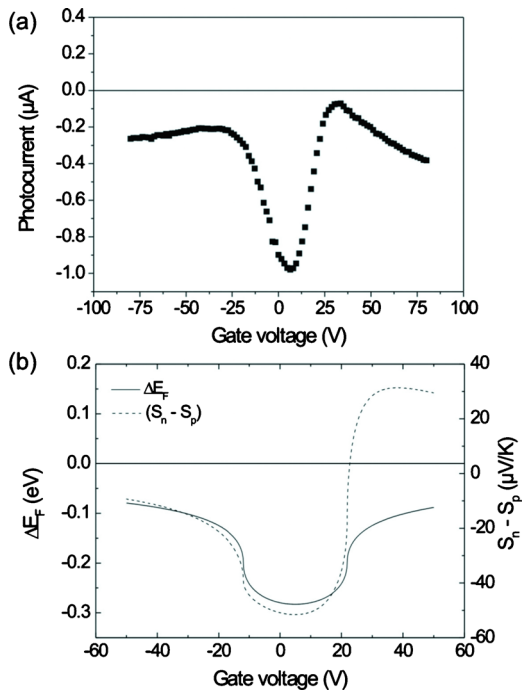

FIG. 3. (Color online) (a) Photocurrent measured at the graphene p-n junction at zero source-drain bias and different gate voltages. (b) Calculated gate dependent Fermi level difference between the n-doped and p-doped graphene sections (full line), and calculated gate dependent difference between the Seebeck coefficients of the n- and p-doped graphene sections (dashed line).

applied gate voltage. As apparent from Fig. 3(b), the photocurrent measured at the p-n junction is well reproduced by the calculated Fermi level difference $\Delta E_F = E_{\text{uncovered},F} - E_{\text{covered},F}$ between the two sheet sections as a function of gate voltage. This finding suggests that the photocurrent is governed by the electric potential step ΔV at the junction interface.[15] For comparison, Fig. 3(b) depicts the response expected on the basis of the photothermoelectric effect (PTE), whereby photoexcited charge carriers would diffuse to the region of largest electronic density of states.[18] In the PTE model, the generated photocurrent is proportional to the temperature gradient across the interface, as well as to the difference in the Seebeck coefficients (S) of the corresponding regions. The latter term is given by the Mott relation as follows:

$$S = -\left.\frac{-\pi^2 k_B^2 T}{3e}\frac{1}{G}\frac{dG}{dV_g}\frac{dV_g}{dE}\right|_{E=E_F}, \tag{2}$$

where k_B is the Boltzmann constant and G is conductance. Accordingly, we estimated the Seebeck coefficients of the p- and n-type regions (S_p and S_n) by using the experimental G versus V_g curves, combined with Eq. (1). The corresponding plot in Fig. 3(b) reveals that the difference $(S_p - S_n)$, which is proportional to the PTE-generated photocurrent, reverses sign around the Dirac point of the p-type region. This behavior is clearly different from the measured photocurrent, which lacks such sign reversal predicted by the PTE model.[25] In Fig. 2(a), small positive photocurrents can be observed in the vicinity of the p-n interface at $V_g = 50$ V, and small negative photocurrents are discernable in other interface regions. In view of the absence of a strong potential step at the p-n junction for this gate voltage, these signals may originate from potential fluctuations associated with charged impurities or defects. It is noteworthy that the emergence of a small positive photocurrent does not contradict the above conclusion, since the PTE model predicts a pronounced, positive photocurrent for $V_g > V_g^{\text{Dirac}}$ comparable to the negative signals observed at the p-n junction.

In summary, the gate dependent photocurrent response of a graphene p-n junction has been found to be dominated by the electric potential step at this location, although a contribution from the PTE cannot be ruled out. The photocurrent maps are thus consistent with the existence of three different, gate controlled device regimes, namely, n^+-n, p-n, and p^+-p. Similar studies on devices comprised of modified graphene with a band gap are promising to explore the suitability of graphene for photodetector or solar cell applications.

The authors are grateful to R. S. Sundaram and B. Krauss for assistance with the Raman measurements.

[1] J. R. Williams, L. DiCarlo, and C. M. Marcus, Science **317**, 638 (2007).
[2] D. A. Abanin and L. S. Levitov, Science **317**, 641 (2007).
[3] B. Özyilmaz, P. Jariloo-Herrero, D. Efetov, D. A. Abanin, L. S. Levitov, and P. Kim, Phys. Rev. Lett. **99**, 166804 (2007).
[4] G. Liu J. Velasco, W.Z. Bao, C.N. Lau, Appl. Phys. Lett. **92**, 203103 (2008).
[5] M. I. Katsnelson, K. S. Novoselov, and A. K. Geim, Nat. Phys. **2**, 620 (2006).
[6] V. V. Cheianov and V. I. Fal'ko, Phys. Rev. B **74**, 041403 (2006).
[7] N. Stander, B. Huard, and D. Goldhaber-Gordon, Phys. Rev. Lett. **102**, 026807 (2009).
[8] A. F. Young and P. Kim, Nat. Phys. **5**, 222 (2009).
[9] R. V. Gorbachev, A. S. Mayorov, A. K. Savchenko, D. W. Horsell, and F. Guinea, Nano Lett. **8**, 1995 (2008).
[10] V. V. Cheianov, V. Fal'ko, and B. L. Altshuler, Science **315**, 1252 (2007).
[11] D. B. Farmer, R. Golizadeh-Mojarad, V. Perebeinos, Y. M. Lin, G. S. Tulevski, J. C. Tsang, and P. Avouris, Nano Lett. **9**, 388 (2009).
[12] D. B. Farmer, Y. M. Lin, A. Afzali-Ardakani, and P. Avouris, Appl. Phys. Lett. **94**, 213106 (2009).
[13] K. Balasubramanian, Y. Fan, M. Burghard, K. Kern, M. Friedrich, U. Wannek, and A. Mews, Appl. Phys. Lett. **84**, 2400 (2004).
[14] E. J. H. Lee, K. Balasubramanian, R. T. Weitz, M. Burghard, and K. Kern, Small **3**, 2038 (2007).
[15] E. J. H. Lee, K. Balasubramanian, R. T. Weitz, M. Burghard, and K. Kern, Nat. Nanotechnol. **3**, 486 (2008).
[16] F. N. Xia, T. Mueller, R. Golizadeh-Mojarad, M. Freitag, Y. M. Lin, J. Tsang, V. Perebeinos, and P. Avouris, Nano Lett. **9**, 1039 (2009).
[17] T. Mueller, F. Xia, M. Freitag, J. Tsang, and P. Avouris, Phys. Rev. B **79**, 245430 (2009).
[18] X. D. Xu, N. M. Gabor, J. S. Alden, A. M. van der Zande, and P. L. McEuen, Nano Lett. **10**, 562 (2010).
[19] J. Park, Y. H. Ahn, and C. Ruiz-Vargas, Nano Lett. **9**, 1742 (2009).
[20] K. S. Novoselov, A. K. Geim, S. V. Morozov, D. Jiang, Y. Zhang, S. V. Dubonos, I. V. Grigorieva, and A. A. Firsov, Science **306**, 666 (2004).
[21] A. C. Ferrari, Solid State Commun. **143**, 47 (2007).
[22] H. E. Romero, N. Shen, P. Joshi, H. R. Gutierrez, S. A. Tadigadapa, J. O. Sofo, and P. C. Eklund, ACS Nano **2**, 2037 (2008).
[23] T. Lohmann, K. von Klitzing, and J. Smet, Nano Lett. **9**, 1973 (2009).
[24] G. Giovannetti, P. A. Khomyakov, G. Brocks, V. M. Karpan, J. van den Brink, and P. J. Kelly, Phys. Rev. Lett. **101**, 026803 (2008).
[25] The Seebeck coefficients were also estimated by using the relation $G = \alpha(V_g - V_g^{\text{Dirac}})e\mu$, where $\alpha = 7.3 \times 10^{10}$ cm^{-2} V^{-1} is the gate coupling parameter and μ is the carrier mobility. In this case, the agreement with experimental data is even poorer, since the difference $(S_p - S_n)$ reverses sign in the region between the Dirac points of the p- and n-type regions.